A ferroelectric polymer introduces addressability in electrophoretic display cells

Negar Sani, Deborah Mirbel, Simone Fabiano, Daniel Simon, Isak Engquist, Cyril Brochon, Eric Cloutet, Georges Hadziioannou, Magnus Berggren

A Ferroelectric Polymer Introduces Addressability in Electrophoretic Display Cells

Negar Sani[1], Déborah Mirbel[2], Simone Fabiano[1], Daniel Simon[1], Isak Engquist[1], Cyril Brochon[2], Eric Cloutet[2], Georges Hadziioannou[2] and Magnus Berggren[1]

[1] Department of Science and Technology, Linköping University, SE-60174 Norrköping, Sweden

[2] Laboratoire de Chimie des Polymères Organiques (LCPO), Université de Bordeaux, CNRS (UMR 5629), INP Bordeaux - Allée Geoffroy Saint Hilaire, Bât B8, CS 50023, 33615 Pessac Cedex, France

Abstract

During the last decades, tremendous efforts have been carried out to develop flexible electronics for a vast array of applications. Among all different applications investigated in this area, flexible displays have gained significant attention, being a vital part of large-area devices, portable systems and electronic labels etc. Electrophoretic (EP) ink displays have outstanding properties such as a superior optical switch contrast and low power consumption, besides being compatible with flexible electronics. However, the EP ink technology requires an active matrix-addressing scheme to enable exclusive addressing of individual pixels. EP ink pixels cannot be incorporated in low cost and easily manufactured passive matrix circuits due to the lack of threshold voltage and non-linearity, necessities to provide addressability. Here, we suggest a simple method to introduce non-linearity and threshold voltage in EP ink display cells in order to make them passively addressable. Our method exploits the non-linearity of an organic ferroelectric capacitor that introduces passive addressability in display cells. The organic ferroelectric material poly(vinylidene fluoride-co-trifluoroethylene) (P(VDF-TrFE)) is here chosen because of its simple manufacturing protocol and good polarizability. We demonstrate that a non-linear EP cell with bistable states can be produced by depositing a P(VDF-TrFE) film on the bottom electrode of the display cell. The P(VDF-TrFE) capacitor and the EP ink cell are separately characterized in order to match the surface charge at their respective interfaces and to achieve and optimize bistable operation of display pixels.

Introduction

With an increasing demand for thin, flexible, light-weight electronics on the market, a major research effort is directed towards developing flexible displays that run at low power consumption protocols and are possible to produce using a simple and low-cost fabrication process [1-7]. Electrophoretic (EP) inks have been considered as one of the candidates for such applications due to their ability to be integrated with

flexible electronics, superior optical properties and low power consumption when incorporated in electrophoretic image displays (EPIDs) [8-10]. The EP ink technology consists of colored charged particles in an inert media that is encapsulated between a rear and a transparent top electrode. Upon applying voltage to the electrodes, the charged particles migrate, according to electrophoresis, towards the electrode with the opposite polarity causing the cell to adopt the color of the particles that accumulate along the transparent top electrode.

A display device consists of individual pixels that are exclusively addressable to enable updating of the image to be displayed. Commonly, matrix addressing is utilized, which is a technology concept that includes pixels that are arranged in a 2D cross-point matrix. Individual pixels are addressed via row and column lines. There are two main approaches for matrix addressing: Active Matrix (AM) and Passive Matrix (PM) addressing. AM addressing is a mature technology that has been used for displays since the first liquid crystal displays were introduced to the market [11]. In an AM display, an active element i.e. a thin film transistor (TFT) is used as a switch in each pixel. PM addressing has a simpler architecture as compared to the AM; the crossing between a row electrode and a column electrode together with the characteristics of the pixel device is utilized to achieve addressability. Since PM does not require any active addressing circuitry in each pixel, it is tempting to consider PM addressing before AM ditto, since a PM addressing circuit is relatively much simpler and enables a fabrication protocol of lower cost. However, addressability in a PM scheme requires pixels with a current-voltage and switching characteristic that is strongly non-linear.

Several approaches have been demonstrated for active matrix addressing of EPIDs among which the technologies based on organic materials are promising due to their compatibility with flexible and printed electronics [12-16]. PM addressing has been used for display technologies that are based on pixel elements that have some intrinsic non-linearity such as light emitting diodes (LEDs) and ferroelectric liquid crystals. However, very few approaches have been reported on utilizing PM addressing in EPIDs [17-19]. In general, it is believed that since EPID pixels do not exhibit an inherent current-voltage threshold they are not good candidates for PM addressing. A possible solution would be to use a non-linear element in combination with the linear EPID pixel in order to introduce the desired threshold characteristics in the current-voltage characteristics of the pixels. Lilja et al. have used two diodes to add nonlinearity in EPIDs, introducing an extra layer of complexity to the system [19]. Here, we report a simple approach to implement non-linear I-V characteristics in IPED pixels using a thin film of an organic ferroelectric polymer.

Ferroelectric polymers belong to a class of materials with permanent electrical dipoles that can gain a stable polarization by applying an electric field. Ferroelectrics are used in a variety of applications including sensors, microsystems, memories and high frequency electrical components [20, 21]. Work on organic

ferroelectrics and their applications started in the 1980s; however, only in the past few years researchers boosted investigating organic ferroelectrics mainly as a solution for downscaling problem of conventional electronic memories [22-24]. Among the ferroelectric polymers, poly(vinylidene fluoride) (PVDF) and its copolymers with the trifluoroethylene (TrFE) moiety have been the center of interest for many research studies [25]. This is due to the particular properties of P(VDF-TrFE) including simple, low temperature and solution-based processing and stability beside the general advantages of organic materials such as being flexible and feasible for large scale manufacturing [24, 25]. P(VDF-TrFE) has been incorporated in ferroelectric capacitors [26, 27], thin film transistors (TFT) [28-30] and diodes [31] intended for energy storage and memory applications and in switching units for passive driving of an organic LED (OLED) matrix [32, 33].

In this work, we show that by connecting a P(VDF-TrFE) capacitor to one of the EPID cell electrodes a threshold voltage can be introduced in the EPID cell current-voltage characteristics making the cell addressable in a PM configuration. In order to obtain bistability in a ferroelectric capacitor, sufficient charge must be provided at the film interface to compensate for the polarization charge along the surface of the ferroelectric [34]. If the layer adjacent to the capacitance, in our case the EP ink, does not provide the compensation charge, the ferroelectric cannot completely polarize. Depending on the ability of the adjacent layer to provide positive and/or negative charges on the surface, one or both of the polarization states can be instable. The surface charge in an EP cell can be characterized by measuring the double layer capacitance formed on the cell electrodes. With this capacitance value at hand, the surface area ratio between the ferroelectric and the EP cell can be adjusted to balance the surface charges along the two interfaces, which encompasses the EP dispersion layer. Here, we have used impedance spectroscopy to measure the double layer capacitance on the EP cell electrodes to estimate the proper surface area ratio. The results from impedance spectroscopy measurement reflects the impedance of the whole cell that is a combination of different impedance contributions, such as the ink resistivity and the contact resistance besides the double layer capacitances. Therefore, an appropriate electrical equivalent circuit is chosen for the cell and the impedance spectroscopy data is analyzed to identify the impedance of the individual circuit components. We demonstrate that with a proper choice of the surface area ratio, a cell with bistable electrical characteristics can be obtained. To the best of our knowledge this is the first time non-linearity is introduced to an EPID cell using a ferroelectric capacitance and also the first time bistable switching of the ferroelectric layer using an EP dispersion is demonstrated.

Method

The synthesis of the macroinitiator PLA_{23}-SG1 is inspired by the work from Charbonnier *et al* [35]. TiO_2@SiO_2 core-shell particles are synthesized following the Stöber process. Silanization of the TiO_2@SiO_2 particles surface is performed with OTS coupling agents leading to TiO_2@SiO_2-OTS [36]. Poly(AA-co-LA_{23}), a macroinitiator and acrylic acid (AA, purchased from Sigma Aldrich) are then polymerized via dispersion polymerization in Isopar G in presence of TiO_2@SiO_2-OTS leading to the creation of hybrid core-shell particles. Dispersion polymerization in Isopar G involves the following steps: TiO_2@SiO_2-OTS is dispersed in Isoparaffin G in a round bottom flask, then AA and macroinitiator is solubilized. This solution is degassed by nitrogen bubbling for 1 hour. After oxygen removal, the solution is heated at 120°C under magnetic stirring (375 rpm) for 15 hours. Once the reaction is complete, the particle dispersion is cooled down and purified by 3 cycles of centrifugation and re-dispersion in Isoparaffin G to remove the residual monomers.

Hybrid particles are charged using tridodecylamine, a basic charge control agent, leading to negatively charged particles with tridodecylamonium counter cations [37]. For the electrophoretic display application 8.8wt% of PED G5 particles and 0.13wt% blue dye oil are mixed into Isopar G solutions to obtain an electrophoretic ink with white/blue states.

For preparing the electrophoretic display cell first a 50 µm Kapton spacer is placed on top of an ITO coated glass bottom electrode and another ITO coated glass is glued on top of the spacer using a Bondic UV curable welder. Then the ink is injected between the electrodes and the cell is sealed using the same welder. An Alpha High Resolution Dielectric Analyze potentiostat is used to conduct the electrochemical impedance spectroscopy (EIS) and the voltage-current measurements are performed using a Keithley 4200-SCS source meter.

The preparation of the ferroelectric capacitors starts with dissolving the P(VDF-TrFE) 70/30 mol % copolymer, purchased from Solvay SA, in diethyl carbonate (DEC) at a concentration of 4 wt%. The solution is then filtered through a 0.45 µm filter. Gold bottom electrodes are deposited on Si substrate via thermal evaporation. To obtain a 140 nm-thick film the 4 wt% P(VDF-TrFE) in DEC solution is spin coated on the gold electrodes on Si wafer with 2000 rpm spin rate for 30 s and annealed in 130 °C for 20 minutes and slowly cooled down to RT. This step is repeated multiple times to obtain thicker layers of P(VDF-TrFE). An aluminum top electrode is then deposited via thermal evaporation.

Results

1. Characterization and modelling of the ink

The EP ink used in this work comprises white negatively charged particles in a blue dyed Isopar G media. The schematic cross section of an EPID pixel is shown in Figure 1(a). The ink is encapsulated between two ITO coated glass electrodes separated with a spacer. When a positive voltage is applied to the top electrode, the negatively charged white particles accumulate along the top electrode causing the pixel to display the white color state. Conversely, when a voltage with opposite polarity is applied the particles migrate towards the bottom electrode making the pixel display the blue color originating from the media. To record the color switching of the cell the measurement setup illustrated in Figure 1(b) is used. In this setup, a red laser beam is pointed at the top ITO coated glass electrode of the cell. The beam is reflected by the surface of the electrode and then recorded by a photodiode. The changes of the current of the photodiode therefore corresponds to the reflective changes of the display pixel color [38]. The measurement is performed in a dark box to avoid any external optical noise. Figure 1(c) shows the cell current and color while a voltage pulse train is applied. The zero point on the color axis represents the color white and one represents blue. The white particles tend to sink down with time, therefore the color of the cell in the neutral state (i.e. 0 V bias) lies closer to the blue state rather than white. The cell has a capacitive response as indicated by the current and voltage profiles vs. time. As can be seen in Figure 1(c), with a voltage pulse with an amplitude of 5 V or above, the cell color can be completely switched between two stable states.

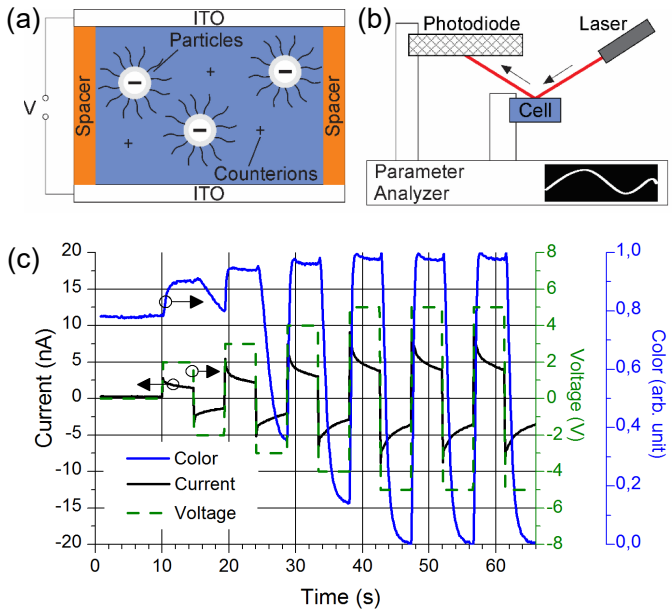

Figure 1 (a) Schematic structure of the EP cell. (b) Measurement setup used to record the color of the cell. (c) The current, the applied voltage and the color of the cell plotted vs. time (in the color axis zero corresponds to the blue state and one corresponds to the white state of the cell).

Impedance spectroscopy is conducted on a 50 µm thick EP cell with 0.3 cm^2 surface area, over the frequency range from 1 to 10^6 Hz (Figure 2). The impedance of the cell reveals the electrical characteristics of the different cell components (i.e. electrodes, ink, connections etc.) and the interaction between them upon application of an electric field. These characteristics and interactions can be modelled using an appropriate electrical equivalent circuit. Assuming a condition where there is no electrochemistry at the cell electrodes, the charges and the charged particles start moving towards the electrodes as the field is applied. This drift of charges can be assigned to a resistance in the equivalent circuit (R_f). As the charges reach the electrodes, they start forming a double layer capacitance on the electrodes that is modelled with a capacitor (C_{dl}) in series with the cell resistance in the equivalent circuit. Another parameter that should be considered is the parallel plate capacitance between the cell electrodes, which can be modelled by a capacitance (C_g) in parallel with R_f and C_{dl}. The connections to the cell for the measurement also add a small contact resistance (R_s) that is configured in series with the cell impedance. The equivalent circuit composed of the described four parameters is illustrated in the inset of Figure 2(a). A similar approach to what Yezer et al. have suggested is taken to extract the values of the model parameters from the impedance spectroscopy data [39]. The values of C_{dl}, R_f, C_g and R_s are estimated to be 20 nF, 1.8x10^8 Ω, 0.5 nF and 400 Ω respectively for a cell with 50 µm thickness and 0.3 cm^2 surface area. The simulation results of the model show a good match with the experimental data as shown in Figure 2.

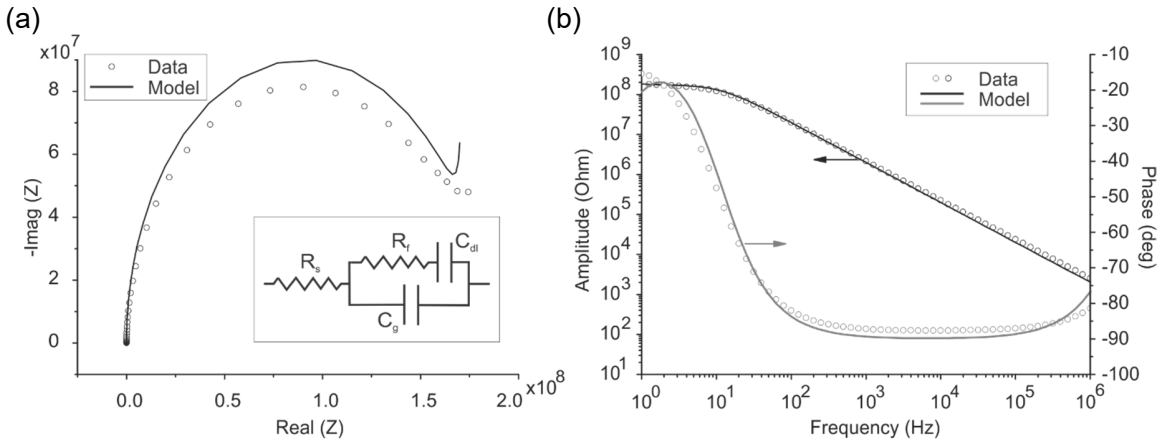

Figure 2 (a) The Nyquist plot of the cell impedance (circles) and the model (solid line). The inset of the left side image shows the electrical equivalent circuit used to model the cell. (b) The amplitude and phase of the cell impedance (circles) and the model (solid line).

2. Characterization of the P(VDF-TrFE) capacitor

P(VDF-TrFE) (see the inset of Figure 3) is the most commonly used organic ferroelectric material with a typical remnant polarization of about 10 μC/cm^2 [40, 41]. In order to polarize a P(VDF-TrFE) film an electric field should be applied across it. The minimum electric field needed for the polarization of the P(VDF-TrFE) is called the coercive field. When the electric field applied across the P(VDF-TrFE) film, increases from zero, the electric dipoles start to align with the field. Close to the coercive field the polarization of the dipoles results in an electric current across the film which peaks at the coercive field and decreases to zero after all the dipoles are aligned. To estimate the coercive field, ~~voltage,~~ ferroelectric capacitors with different thicknesses are fabricated and the polarization voltage is measured. Figure 3(a) shows the polarization voltage of ferroelectric capacitors vs. thickness. The coercive ~~voltage~~ field is calculated from the slope of the line to be approximately ~~around~~ 91 MV/m which is in good agreement with previously reported values [40]. The I-V characteristics of a P(VDF-TrFE) capacitor with an Au electrode and an Al electrode sandwiching a 280-nm-thick polymer ferroelectric layer is shown in Figure 3(b).

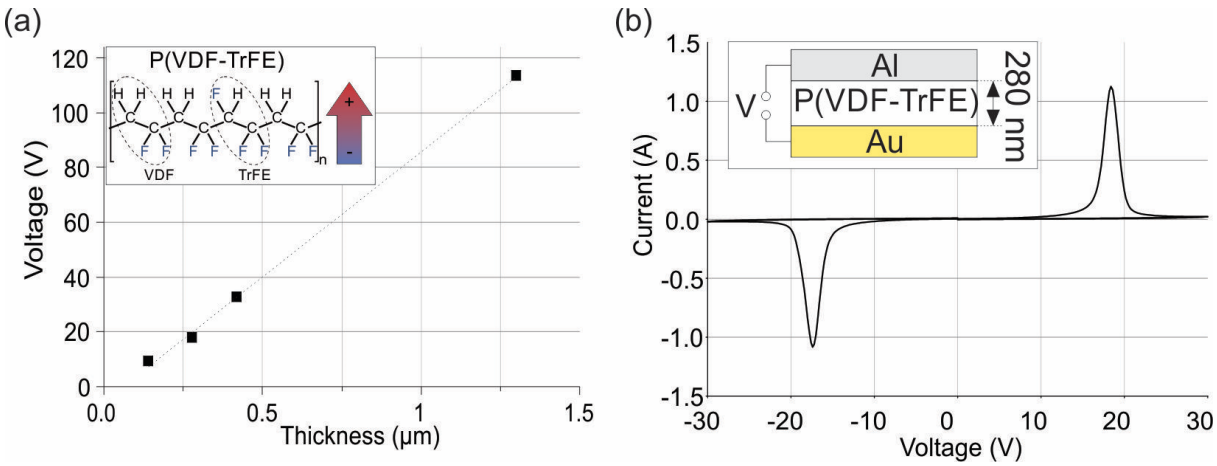

Figure 3 (a)The polarization voltage of the P(VDF-TrFE) vs. the film thickness. The inset shows the molecular structure of P(VDF-TrFE). (b) The 10 V/s I-V curve of a 280 nm P(VDF-TrFE) capacitor in the inset with the coercive voltage of about 16 V.

3. The integrated device

As discussed before, an electrophoretic display has a linear capacitive current-voltage relation and the voltage needed for switching of the color depends on the cell thickness. A non-linear element is needed to provide a threshold voltage of the cell. Here the ferroelectric capacitor is used as a passive non-linear element to set the threshold voltage for switching of the display color. The structure of the display cell integrated with the ferroelectric capacitance is schematically shown in Figure 4(a1). However, for all of the

measurements and characterizations, the setup in Figure 4(a2) is actually used. This configuration is in fact the exact equivalent of the integrated cell.

In order to switch the polarization of the ferroelectric capacitor an equal amount of compensation charge should be available on the electrodes otherwise the ferroelectric layer depolarizes. As shown in Figure 1(c), the color of the EP cell with 50 µm thickness is completely switched at ±5 V. At a steady state condition, under electric bias, the surface charge on the electrodes equals the product of C and V, where C is the sum of C_{dl} and C_g. For a cell biased at 5 V with 1 cm^2 surface area this calculation gives a value about 330 nC. Therefore, in order to provide the compensation charge for the polarization of the ferroelectric (10 $\mu C/cm^2$) the surface area of the EP cell must be at least 30 times larger than that of the ferroelectric [34].

However, in reality the true equivalent circuit of the EP cell appears more complicated since the cell cannot be perfectly modelled using ideal capacitors and resistors. Therefore, an optimum surface area ratio for the actual physical device to work properly might be larger or smaller than the calculated value. Nevertheless, the calculation can be used as a starting point to balance the areas of the top transparent electrode and the area of the ferroelectric device. The calculation indicates that the surface charge per unit area that the electrophoretic ink can provide is about two orders of magnitude less than that of the ferroelectric surface. In order to find the optimum surface area ratio between the ferroelectric capacitor and the cell (A_{FE}/A_{EP}), three different surface area ratios, 1/30, 1/125 and 1/500 were tested. Among these three A_{FE}/A_{EP} ratios, 1/125 yields the best result, suggesting a reasonable error in our calculations. Figure 4(b) shows the current of the device vs. the applied voltage while the display color is recorded using the setup shown in Figure 1(b) for a ferroelectric capacitance with 1 mm^2 surface area and 280 nm thickness coupled to a display cell with 1.25 cm^2 surface area. Starting from 0 V when the ferroelectric is not polarized, the current of the device remains low until the coercive field is reached. As soon as the voltage drop on the ferroelectric capacitor reaches the coercive voltage, the ferroelectric is polarized and the charge displacement current flows in the device allowing the charged particles in the display to move and change the display color (Figure 4 (a3)). Once the ferroelectric is polarized, the current drops, and the ~~polarization is maintained~~ferroelectric layer remains polarized until the coercive voltage with the opposite polarity is applied (Figure 4 (a4)). The color of the display switches simultaneously with the current peak in the I-V curve, which means that the ferroelectric polarizes.

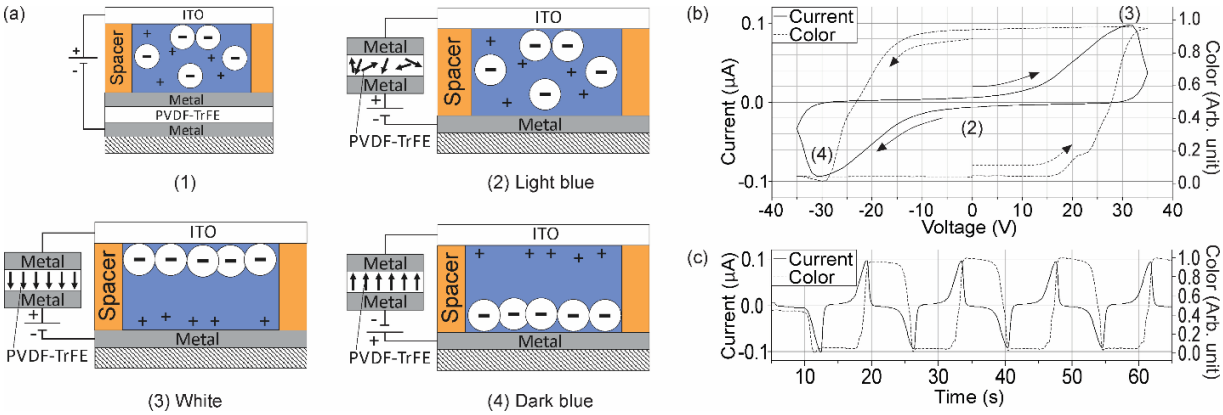

Figure 4 (a1) The structure of the designed electrophoretic cell integrated with the ferroelectric capacitor. (a2) The equivalent circuit of the integrated cell that is used for the measurements before polarizing. (a3,4) The measurement circuit when the ferroelectric is positively and negatively polarized. (b) The current and the color of the device (with a 280-nm-thick ferroelectric) vs. the applied voltage (in the color axis zero corresponds to the blue state and one corresponds to the white state of the cell). -(c) Color and the current of the setup plotted vs. time.

The capacitance of the P(VDF-TrFE) is field dependent and has a maximum at the coercive field. This trend can be observed in the current and voltage profile of the device in Figure 5(a), which shows the current and voltage drop on the ferroelectric capacitanc (a) (b) the EP cell separately. The current peak is an identification of the switching of the ferroelectric polarization. Since the voltage is proportional to the inverse of the capacitance, a large portion of the input voltage drops over the ferroelectric capacitance before and after the polarization when the capacitance is low. During the polarization, the voltage drop on the EP cell has a peak and the input voltage is divided almost equally between the EP cell and the FE capacitor. Figure 5(b) shows the color of the EP cell when a pulse train with levels below and above the coercive voltage is applied. The color of the display remains almost constant as long as the voltage drop on the ferroelectric is below the coercive voltage. Once the coercive field is applied the color changes.

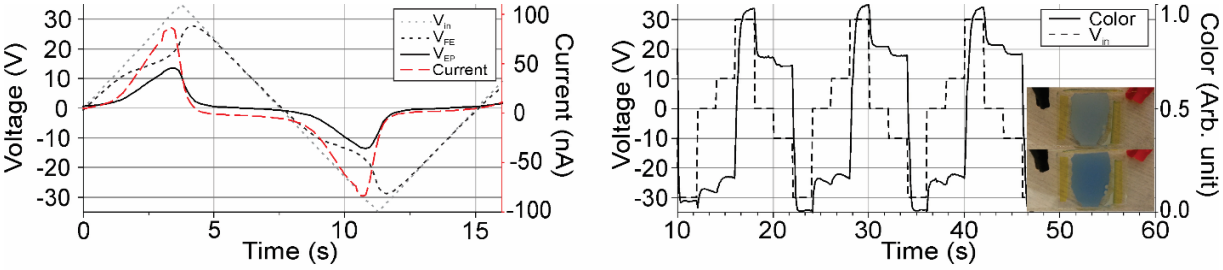

Figure 5 (a) The current, input voltage and the voltage drop on the EP cell and on the ferroelectric capacitor vs. time. (b) The color of the cell while the input pulse train with amplitudes higher and lower than the coercive voltage of ferroelectric are applied (in the color axis zero corresponds to the blue state and one corresponds to the white state of the cell). The inset shows the two-color states of the EP cell.

In case the surface area ratio A_{FE}/A_{EP} is larger than the optimum value, the display cannot provide enough surface charge to compensate for the remnant polarization of the ferroelectric. To exemplify this, the electrical and the color profile of an EP cell with 1.25 cm^2 surface area connected to a 4 mm^2 P(VDF-TrFE) capacitor ($A_{FE}/A_{EP} \approx 1/30$) is shown in Figure S1. Increasing the surface area of the ferroelectric cell results in higher ferroelectric capacitance and leakage current. Consequently, the voltage drop on the EP cell is higher and the leakage current of the ferroelectric allows the charged particles in the display to move and the display color switches. However, the voltage drop on the ferroelectric does not reach the coercive voltage and the ferroelectric does not polarize.

A small surface area ratio A_{FE}/A_{EP}, has an opposite effect in that the ferroelectric capacitance polarizes completely, but the color of the EP cell does not completely switch. Figure S2 shows the electrical and the color profile of an EP cell with 1.25 cm^2 surface area connected to a 0.25 mm^2 P(VDF-TrFE) capacitor ($A_{FE}/A_{EP} \approx 1/500$). In this case, there are more than enough surface charges available in the display to compensate for the remnant polarization of the ferroelectric. The capacitance and the current leakage of the ferroelectric are lower resulting in a larger portion of the input voltage to fall over the ferroelectric. Therefore, once the coercive field is applied, the ferroelectric completely polarizes. However, a smaller ferroelectric surface area results in a smaller charge displacement current. The current is not high enough to allow all the charged particles to move to the electrode with opposite polarity and the display cannot switch the color completely. This effect is clearly illustrated in Figure S2(b) showing the EP cell color vs. time when a voltage sweep is repeatedly applied. The color levels in different cycles are not stable since the current is not enough to allow all of the charged particles to move.

Conclusion

In summary, we present a simple approach to define a threshold voltage for an electrophoretic display cell by depositing a layer of the organic ferroelectric P(VDF-TrFE) on one of the electrodes of the cell. As a first step, the electrophoretic ink is characterized using impedance spectroscopy and modelled with an electrical equivalent circuit to estimate the capacitance and consequently the surface charge density of the display cell. The surface area ratio between the ferroelectric and the display cell is balanced so that the electrophoretic ink can provide enough surface charge to polarize the ferroelectric thin film. The ferroelectric displacement current is just enough for the display to fully switch the color. We have used the electrical equivalent of non-linear EP cell structure to show that a threshold voltage is added to the I-V characteristic of the electrophoretic cell by addition of a ferroelectric layer, meaning that the color of the cell does not change unless the input voltage overcomes the coercive voltage of the ferroelectric layer. This

non-linearity in the device characteristics makes the reported device suitable for passive addressing, which is a simple and low-cost alternative to the active addressing configuration commonly used for EPIDs.

Acknowledgements

This research was partially supported by the Advanced Functional Materials Center at Linköping University and the Önnesjö Foundation. The authors thank the Knut and Alice Wallenberg Foundation (Power Paper project, scholar) and the Swedish Foundation for Strategic Research (Synergy project) for financial support.

We would like to thank ARKEMA for the blocbuilder-SG1® and the Aquitaine region for the funding. The authors thank Arkema for the CIFRE PhD fellowship allocated to D.M. This work was performed within the framework of the Equipex ELORPrintTec ANR-10EQPX-28-01 and the LabEx AMADEUS ANR-10-LABEX0042-AMADEUS with the help of the French state Initiative d'Excellence IdEx ANR-10-IDEX-003-02 and the LCPO/ Arkema INDUSTRIAL CHAIR "HOMERIC" ANR-13CHIN-0002-01.

References

1. Andersson Ersman, P., J. Kawahara, and M. Berggren, *Printed passive matrix addressed electrochromic displays.* Organic Electronics, 2013. **14**(12): p. 3371-3378.
2. Tehrani, P., et al., *Improving the contrast of all-printed electrochromic polymer on paper displays.* Journal of Materials Chemistry, 2009. **19**(13): p. 1799-1802.
3. Gelinck, G.H., et al., *Flexible active-matrix displays and shift registers based on solution-processed organic transistors.* Nat. Mater., 2004. **3**: p. 106-109.
4. Liang, J., C. Jiang, and W. Wu, *Toward fiber-, paper-, and foam-based flexible solid-state supercapacitors: electrode materials and device designs.* Nanoscale, 2019. **11**(15): p. 7041-7061.
5. Liu, L., Y. Feng, and W. Wu, *Recent progress in printed flexible solid-state supercapacitors for portable and wearable energy storage.* Journal of Power Sources, 2019. **410-411**: p. 69-77.
6. Wu, W., *Inorganic nanomaterials for printed electronics: a review.* Nanoscale, 2017. **9**(22): p. 7342-7372.
7. Wu, W., *Stretchable electronics: functional materials, fabrication strategies and applications.* Science and Technology of Advanced Materials, 2019. **20**(1): p. 187-224.
8. Heikenfeld, J., et al., *Review Paper: A critical review of the present and future prospects for electronic paper.* Journal of the Society for Information Display, 2011. **19**(2): p. 129-156.
9. Comiskey, B., et al., *An electrophoretic ink for all-printed reflective electronic displays.* Nature, 1998. **394**(6690): p. 253-255.
10. Chen, Y., et al., *Electronic paper: Flexible active-matrix electronic ink display.* Nature, 2003. **423**(6936): p. 136-136.
11. Kawamoto, H., *The history of liquid-crystal displays.* Proceedings of the IEEE, 2002. **90**(4): p. 460-500.
12. Henzen, A., et al., *Development of active-matrix electronic-ink displays for handheld devices.* Journal of the Society for Information Display, 2004. **12**(1): p. 17-22.
13. Burns, S.E., et al., *A scalable manufacturing process for flexible active-matrix e-paper displays.* Journal of the Society for Information Display, 2005. **13**(7): p. 583-586.
14. Gelinck, G.H., et al., *Flexible active-matrix displays and shift registers based on solution-processed organic transistors.* Nat Mater, 2004. **3**(2): p. 106-110.
15. Kawase, T., et al., *Inkjet printing of polymer thin film transistors.* Thin Solid Films, 2003. **438–439**: p. 279-287.
16. Edzer, H., et al., *Flexible electronic-paper active-matrix displays.* Journal of the Society for Information Display, 2006. **14**(8): p. 729-733.
17. Park, J. and J.M. Jacobson. *All printed bistable reflective displays: Printable electrophoretic ink and all printed Metal-Insulator-Metal Diodes*. in *Materials Research Society Symposium - Proceedings*. 1998.
18. Bert, T., et al. *Passive matrix addressing of electrophoretic image display*. in *22nd International Display Research Conference (IDRC 2002/Eurodisplay 2002)*. 2002. Society for Information Display (SID).
19. Lilja, K.E., et al., *Printed organic diode backplane for matrix addressing an electrophoretic display.* Thin Solid Films, 2010. **518**(15): p. 4385-4389.
20. Scott, J.F. and C.A. Paz De Araujo, *Ferroelectric memories.* Science, 1989. **246**(4936): p. 1400-1405.
21. Setter, N., et al., *Ferroelectric thin films: Review of materials, properties, and applications.* Journal of Applied Physics, 2006. **100**(5): p. 051606.
22. Yagi, T., M. Tatemoto, and J.-i. Sako, *Transition behavior and dielectric properties in trifluoroethylene and vinylidene fluoride copolymers.* Polymer Journal, 1980. **12**(4): p. 209-223.
23. Yamauchi, N., *METAL-INSULATOR-SEMICONDUCTOR (MIS) DEVICE USING A FERROELECTRIC POLYMER THIN FILM IN THE GATE INSULATOR.* Japanese Journal of Applied Physics, Part 1: Regular Papers & Short Notes, 1986. **25**(4): p. 590-594.
24. Ling, Q.-D., et al., *Polymer electronic memories: Materials, devices and mechanisms.* Progress in Polymer Science, 2008. **33**(10): p. 917-978.
25. Mai, M., et al., *Ferroelectric Polymer Thin Films for Organic Electronics.* Journal of Nanomaterials, 2015. **2015**: p. 14.
26. Xu, H., et al., *Ferroelectric and switching behavior of poly(vinylidene fluoride-trifluoroethylene) copolymer ultrathin films with polypyrrole interface.* Applied Physics Letters, 2007. **90**(9): p. 092903.
27. Li, X., et al., *P(VDF-TrFE) ferroelectric nanotube array for high energy density capacitor applications.* Physical Chemistry Chemical Physics, 2013. **15**(2): p. 515-520.
28. Fabiano, S., X. Crispin, and M. Berggren, *Ferroelectric Polarization Induces Electric Double Layer Bistability in Electrolyte-Gated Field-Effect Transistors.* ACS Applied Materials & Interfaces, 2014. **6**(1): p. 438-442.
29. Zheng, Y., et al., *Gate-controlled nonvolatile graphene-ferroelectric memory.* Applied Physics Letters, 2009. **94**(16): p. 163505.
30. Sekitani, T., et al., *Printed Nonvolatile Memory for a Sheet-Type Communication System.* Electron Devices, IEEE Transactions on, 2009. **56**(5): p. 1027-1035.

31. Asadi, K., et al., *Organic non-volatile memories from ferroelectric phase-separated blends.* Nat Mater, 2008. **7**(7): p. 547-550.
32. Naber, R.C.G., et al., *Organic Nonvolatile Memory Devices Based on Ferroelectricity.* Advanced Materials, 2010. **22**(9): p. 933-945.
33. Asadi, K., P.W.M. Blom, and D.M. De Leeuw, *The MEMOLED: Active addressing with passive driving.* Advanced Materials, 2011. **23**(7): p. 865-868.
34. Fabiano, S., et al., *Ferroelectric polarization induces electronic nonlinearity in ion-doped conducting polymers.* Science Advances, 2017. **3**: p. e1700345.
35. Charbonnier, A., et al., *Synthesis of functional polymer particles by dispersion polymerization in organic media: A tool toward stable electrophoretic inks.* Journal of Polymer Science Part A: Polymer Chemistry, 2013. **51**(21): p. 4608-4617.
36. Stöber, W., A. Fink, and E. Bohn, *Controlled growth of monodisperse silica spheres in the micron size range.* Journal of Colloid and Interface Science, 1968. **26**(1): p. 62-69.
37. Noel, A., et al., *Tridodecylamine, an efficient charge control agent in non-polar media for electrophoretic inks application.* Applied Surface Science, 2018. **428**: p. 870-876.
38. Kawahara, J., et al., *Improving the color switch contrast in PEDOT:PSS-based electrochromic displays.* Organic Electronics, 2012. **13**(3): p. 469-474.
39. Yezer, B.A., et al., *Use of electrochemical impedance spectroscopy to determine double-layer capacitance in doped nonpolar liquids.* Journal of colloid and interface science, 2015. **449**: p. 2-12.
40. Kliem, H. and R. Tadros-Morgane, *Extrinsic versus intrinsic ferroelectric switching: experimental investigations using ultra-thin PVDF Langmuir–Blodgett films.* Journal of Physics D: Applied Physics, 2005. **38**(12): p. 1860.
41. Ferris, R.J., et al., *Electric Double Layer Formed by Polarized Ferroelectric Thin Films.* Acs Applied Materials & Interfaces, 2013. **5**(7): p. 2610-2617.